

Cite this: *Chem. Commun.*, 2012, **48**, 7003–7018

www.rsc.org/chemcomm

## FEATURE ARTICLE

# Individual nanostructured materials: fabrication and surface-enhanced Raman scattering

Xiao Gong, Ying Bao, Chao Qiu and Chaoyang Jiang\*

Received 3rd March 2012, Accepted 14th May 2012

DOI: 10.1039/c2cc31603j

The progress of surface-enhanced Raman scattering (SERS) microscopy and spectroscopy on individual nanostructured materials has been reviewed in this *feature article*. After a brief introduction on individual nanomaterial SERS, we provide a systematic overview on the fabrication and SERS studies of individual nanoparticulates, nano-junctions and hierarchical nano-aggregate. These SERS-active nanomaterials have great potential in designing novel highly sensitive SERS substrates for the development of SERS-based sensing devices with a broad range of applications.

## 1. Introduction

Nanomaterials have demonstrated unique physical and chemical properties due to the quantum confinement that is associated with their nanometer scale dimensions. A variety of top-down and bottom-up methods have been used to fabricate nanomaterials, while it is still quite challenging to synthesize nanostructures with uniform size, shape and crystallinity. Consequently, nanomaterial characterization can be conducted with a focus on either collective properties or the properties of individual nanostructures. A detailed characterization on individual nanomaterials can reveal additional properties regarding their structure–property relationship, thus allowing us to design nanostructured materials with better performances.

Optical studies on individual nanomaterials have received increasing interest in recent years due to the broad

applications of nanomaterials in the fields of plasmonics and nanophotonics.<sup>1–5</sup> For example, the factors that influence the line width of the localized surface plasmon resonance (LSPR) for single metal nanoparticles have been studied with dark-field optical microscopy.<sup>3</sup> Similarly, confocal white light reflection microscopy has been utilized to image individual metallic nanostructures.<sup>6</sup> Combining LSPR spectroscopy and high-resolution transmission electron microscopy (HRTEM), Schatz and co-workers investigated the optical response and structural information on a single silver nanocube.<sup>1</sup> Recently, Guo and co-workers developed a reusable aptasensor using a single gold nanorod and successfully detected analytes with an excellent sensitivity and reproducibility.<sup>4</sup> In all these experiments, optical microscopes were generally used to locate and identify the individual nanostructures.

Surface-enhanced Raman scattering (SERS) spectroscopy on individual nanostructures has emerged as a new active field to understand the SERS mechanism and to develop novel SERS substrates with superior enhancement. Raman spectroscopy has been widely used in characterizing molecular structures

Department of Chemistry, University of South Dakota, Vermillion, South Dakota, 57069, USA. E-mail: Chaoyang.Jiang@usd.edu; Fax: +1 605 677 6397; Tel: +1 605 677 6250



Xiao Gong

Xiao Gong received his PhD Degree from Zhejiang University, China in 2009. He joined the University of Houston as a Postdoc Fellow in 2010. He is currently a postdoctoral research associate in the group of Prof. Jiang at the University of South Dakota. His current research interests include nanomaterials synthesis and assembly, plasmonics and development of nanomaterial-based surface-enhanced Raman scattering substrates.



Ying Bao

Ying Bao received her Bachelor of Engineering Degree in Pharmaceutical Engineering from Zhejiang Chinese Medical University, China, in 2008. In 2010, she received her Master of Science Degree in Chemistry under the supervision of Prof. Chaoyang Jiang at the University of South Dakota. Since then she has been pursuing her PhD degree in the same institute. Her current research interest focuses on fabrication and utilization of plasmonic nanocomposites.

of nanostructured materials,<sup>7</sup> such as carbon nanotubes.<sup>8,9</sup> Furthermore, Raman spectroscopy has also been extensively used to assess the performance of novel plasmonic nanostructures as SERS substrates. The exploration of SERS theories and fabrication of functional nanomaterials have clearly demonstrated the great potential for the SERS technique, which range from photodetection, single molecular experiments and biomaterial sensing to chemical identification.<sup>10–13</sup> While it has been well-recognized that both electromagnetic and chemical mechanisms contribute to the enhancement in the SERS experiments, a unified SERS expression was proposed recently by Lombardi and Birke, which contains three denominators representing the surface plasmon resonance, the metal–molecule charge-transfer resonance and molecular resonance, respectively.<sup>14</sup> In addition, the authors demonstrated that those three resonances were linked by Herzberg–Teller vibronic coupling terms and should be considered simultaneously.<sup>15</sup>

It is well-known that the SERS activities for certain nanostructured substrates largely depend on the activity and density of Raman hot spots.<sup>16</sup> However, most SERS evaluations were conducted on random locations of a SERS substrate. With inhomogeneous substrates, it can be very difficult to obtain valuable structural information for further material optimization. The appearance of single-particle SERS (sp-SERS), on the other hand, provides an ideal solution for such a problem. sp-SERS experiments can not only allow detailed studies on structure–property relationship for individual nanostructures, but also provide a great opportunity for structural optimization of the nanomaterials, thus promoting the fabrication of novel SERS-active substrates with unprecedented SERS activities.

Single-particle SERS focuses on collecting SERS signals from individual particles, and in most cases, these individual particles are nanostructured materials. sp-SERS, together with the SERS experiments from individual assemblies and aggregates provides an excellent opportunity to understand the structure–SERS performance relationship of these individual nanostructures, thus providing a guideline to design SERS-active materials with exceptional sensitivities. Initially, most

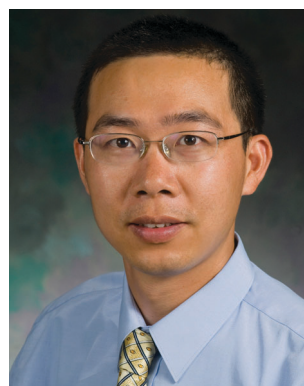
sp-SERS reports were limited to single-molecular SERS spectroscopy. In 1997, Nie and Emory studied SERS spectra of individual rhodamine 6G (R6G) molecules on isolated silver colloidal nanoparticles and they demonstrated that intrinsic Raman enhancement factors were much larger than the ensemble-averaged values with conventional methods.<sup>17</sup> The chemical enhancement effect in sp-SERS was later studied in detail and spectral blinking was examined.<sup>18–20</sup> Furthermore, they studied sp-SERS by using near-field Raman microscopy where individual metallic nanoparticles were attached to near-field fiber probes to create Raman hot spots.<sup>21</sup> In 1999, Brus and co-workers observed strong SERS signals for individual R6G molecules on large silver nanoparticles.<sup>22</sup> Their results were consistent with Nie's studies, and the huge SERS intensities, they believed, originated from the interaction between the chemisorbed molecules and ballistic electrons in optically excited silver nanoparticles. The pioneering work in the late 1990s has resulted in tremendous research interests and experimental investigations in the sp-SERS field. For example, Willets and co-workers introduced a new approach of so-called super-resolution optical imaging and studied the interaction between probe molecules and single nanoparticle hot spots within a diffraction-limited spot.<sup>23</sup>

This feature article will be focused on sp-SERS and SERS of individual nanostructure assemblies, with most of examples of non-single molecular SERS. For those who are interested in single-molecular SERS, there have been several excellent reviews on that topic.<sup>24–28</sup> We will focus on SERS studies that are related to substrates with individual nanostructures and isolated nanoscale aggregates. In this article, we will make a brief review of localized Raman mapping and spectroscopy on SERS active substrates with individual nanostructures and their assemblies. SERS discussion will be based on the types of the substrates, including individual nanoparticles, nanoscale junctions, and nano-aggregations (Fig. 1). These discussions will be followed by brief descriptions for the applications of sp-SERS and SERS of individual assemblies, current challenges and possible future directions.



**Chao Qiu**

*Chao Qiu received his Bachelor of Science Degree in Materials Chemistry from Qingdao University of Science and Technology, China, in 2009. He joined Dr Chaoyang Jiang's research group at the University of South Dakota and received his Master of Science Degree in Chemistry in 2011. Since then he has been pursuing his PhD degree in the same institute. His current research interest focuses on various plasmonic nanomaterial syntheses and applications.*



**Chaoyang Jiang**

*Chaoyang Jiang received his BS Degree in 1996 and his PhD Degree in 2000 from Nanjing University, China. From 2000 to 2007, he had his postdoctoral training in Johannes Gutenberg University Mainz, Germany, Iowa State University, and Georgia Institute of Technology. He joined the Department of Chemistry at the University of South Dakota as an Assistant Professor in 2007. His current research interests include layer-by-layer assembly, metallic nanostructures, plasmonic nanocomposites and surface-enhanced Raman scattering.*

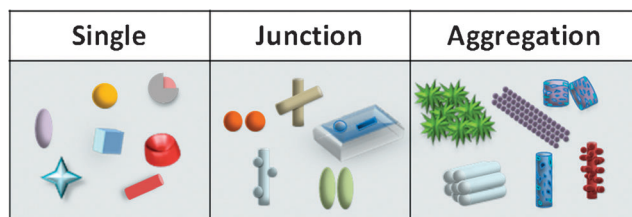


**Fig. 1** Schematic of three types of individual nanostructures for SERS experiments: single nanoparticulates, junctions and aggregations.

## 2. SERS on individual nanoparticulates

While most SERS studies are on bulky nanomaterial aggregates, it is essential to investigate SERS of individual nanoparticulates. A better understanding of the SERS mechanism from individual nanoscale building blocks will help in the design of novel SERS-active substrates. Here, individual nanomaterials can be classified into four categories according to their dimensions: zero-dimensional (0D), one-dimensional (1D), two-dimensional (2D), and three-dimensional (3D) nanomaterial.

### 2.1 Zero-dimensional nanomaterials

Nanoparticles, namely 0D nanomaterials, have been widely used as SERS substrates. Noble metals, such as gold and silver, have a long history of being used in the form of nanoparticle assemblies or roughened surfaces for SERS active substrates. Recently, transition metals and semiconductors also emerged as active substrates in SERS studies. In the field of sp-SERS, the structures of zero-dimensional nanomaterials can be solid nanoparticles, hollow nanoparticles or core-shell nanoparticles.

**Solid nanoparticles.** Solid nanoparticles are the simplest nanomaterials that have been intensively studied. Recently, there has been increasing interests on SERS enhancement from individual nanoparticles of noble metals.<sup>17,19</sup> Furthermore, nanoparticles with various sizes and shapes exhibit tunable optical properties, and such optical characteristics can have a strong impact on the SERS performance. The size-dependent SERS activities from individual silver nanoparticles were reported by Nie's group in 1998.<sup>29</sup> Their experiments revealed that the 488 nm-excited particles have a size about 70 nm, 568 nm-excited particles have a size of 140 nm, and 647 nm laser can excite silver nanoparticles with a size of 190–200 nm. In summary, they found a linear relationship between particle size and excitation wavelength in the SERS experiments.<sup>29</sup>

Besides the size, the shape of individual nanoparticles can also have an important effect on their individual SERS performance. Xia and co-workers systematically examined the effect of nanoparticle shape on the sp-SERS activity.<sup>30</sup> Three types of nanoparticles with different shapes were compared: bipyramid nanoparticles, nanocubes with sharp corners, and truncated nanocubes. As shown in Fig. 2, it is clear that the nanocubes with sharp corners and the bipyramid nanoparticles produced similar Raman intensity, while the truncated nanocubes produced a stronger Raman intensity. If the nanocubes were further truncated, a much stronger Raman intensity could be observed as compared to the spectra

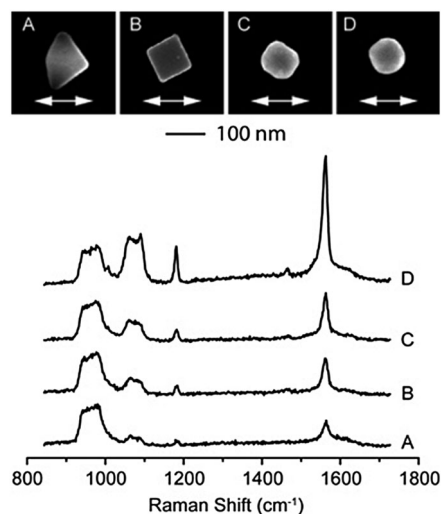


**Fig. 2** SERS spectra of 1,4-benzenedithiol adsorbed on individual Ag nanoparticles with different shapes: (A) bipyramid nanoparticle, (B) nanocube with sharp corners, and (C, D) increasingly truncated nanocubes. Top: corresponding SEM images. Reprinted with permission from ref. 30. Copyright 2007, American Chemical Society.

from the less truncated ones. The authors also found different SERS responses to the polarized excitation on these 0D nanomaterials, and the nanocubes with sharp corners exhibited the largest variation as compared to the others.<sup>30</sup> Such a difference can be due to the difference in the near-field distributions of the electromagnetic field, as proved by both far- and near-field calculations.<sup>30</sup> With a precise control on the shapes of these nanoparticles, their results clearly demonstrated the shape-dependent SERS performances, which are critical in designing novel substrates with superior SERS activities. Similarly, Yang and co-workers reported sp-SERS on silver nanoparticles with unique structures prepared by an anisotropic etching method.<sup>31</sup> In their work, a shape-dependent SERS enhancement was observed on these etched nanoparticles. These nanoparticles might be incorporated into future sensing devices for the simultaneous detections of multiple analytes.

**Hollow nanoparticles.** Single-particle SERS on hollow nanoparticles have been studied and their applications in pH sensing and molecular sensing were explored. Hollow nanoparticles, also denoted nanoshells, are a unique type of 0D nanomaterials. In 2006, a SERS measurement was conducted by Taley's group on single hollow nanostructures.<sup>32</sup> They fabricated hollow gold nanospheres with diameters as small as ~30 nm *via* a galvanic replacement reaction on cobalt nanoparticles. Compared to standard silver nanoparticle aggregates, these hollow gold nanoparticles had a significantly increased SERS intensity of nearly 10-fold. Such strong SERS signals resulted in improved sensitivity and dynamic range for the application of pH sensing. Halas *et al.* fabricated core-shell nanoparticles with a silica core and gold shell.<sup>33</sup> Compared to solid nanospheres, these individual nanoshells provided larger SERS enhancements. It was found that the SERS intensities of the individual nanoshells can be the same order of magnitude strong as that of an individual solid gold nanosphere dimers.

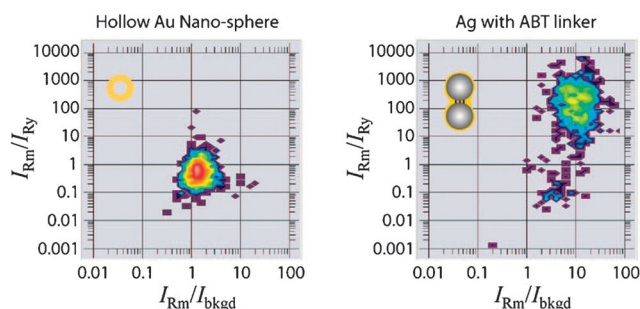


**Fig. 3** The ratios of Raman and Rayleigh scattering strengths to the ratios of Raman signal to background for Au nanospheres (left) and Ag nanoparticles (right). Reprinted with permission from ref. 34. Copyright 2009, American Chemical Society.

Another SERS comparison of hollow nanoparticles and solid nanospheres was reported by Laurence and co-workers, where they used a solution-based single-particle technique to statistically study the uniformity of SERS-active substrates.<sup>34</sup> By plotting the ratios of Raman and Rayleigh scattering strengths to the ratios of Raman signal to background of individual nanostructures (as shown in Fig. 3), a 2D histogram can be obtained to evaluate the SERS intensity of these nanostructures. The narrower the spots are; the more uniform the SERS nanostructures are, due to less variation of the signals. In their experiments, they deduced that the hollow gold nanospheres showed more homogeneous responses as compared to solid gold or silver nanoparticles.<sup>34</sup> Their method can be used to characterize a large number of individual SERS nanoparticles in a very short time, thus providing an efficient approach to examine the quality and uniformity of SERS-active nanoparticles.

Jiang and co-workers recently reported single-particle SERS on individual cuprous oxide ( $\text{Cu}_2\text{O}$ ) nanoshells and systematically investigated the porosity effect of the nanoshells on SERS intensity.<sup>35</sup> In an earlier report, Wang *et al.* reported the syntheses of porous  $\text{Cu}_2\text{O}$  nanoshells and their tunable optical properties.<sup>36</sup> The SERS results on individual nanoshells indicated that strongest SERS were obtained on porous  $\text{Cu}_2\text{O}$  nanoshells with a 30 min Ostwald ripening process.<sup>35</sup> Further treatment could lead to more porous nanoshells and collapsed structures, which reduced the optical scattering at the laser excitation, thus resulting in a decrease of the SERS intensity.<sup>35</sup>

**Core-shell nanoparticles.** Compared with solid nanoparticles and hollow nanoparticles, core-shell nanoparticles have several advantages, such as tunable core diameter and shell thickness, protection of adsorbing analytes by the shell, *etc.* All these allow an optimization and improvement of SERS intensity and reliability. With multiple synthetic steps, core-shell nanoparticles can be fabricated and the shell thickness of core-shell nanoparticles can be adjusted by the temperature, salt, pressure and pH *etc.* The changes on shell thickness might be monitored with SERS tests, thus making the core-shell nanoparticles ideal nanomaterials for sensitive SERS detection. sp-SERS studies on core-shell nanoparticles have been reported with either polymer-metal core-shell nanoparticles or silica-metal core-shell nanoparticles.

Polymer-metal core-shell nanoparticles fabricated from the templates of polymer beads have been studied in sp-SERS for years. To facilitate the core-shell nanoparticle synthesis, the surface of polymer beads were usually chemically modified with functional groups. Silver nanoshells were prepared on the surface of carboxylate-modified polystyrene latex beads.<sup>37</sup> Similarly, Chung *et al.* fabricated gold shells on the surface of amine-terminated polystyrene beads.<sup>38</sup> The thickness of gold nanoshells could be finely tuned by varying the number of electroless plating steps. It was found that SERS activity strongly depended on the number of such steps. Certain encapsulation methods were reported in the literature to improve the SERS performances such as coating a polymer layer to protect the nanoparticles against the surrounding medium. For example, 2-naphthalenethiol analyte was successfully encapsulated between the silver nanoparticle surface and the polymer shell, and the SERS behaviour was studied.<sup>39</sup> Furthermore, the polarization-dependent sp-SERS experiments on polymer-coated silver nanoparticles were also investigated.<sup>39</sup>

Silica can be used as either a core template or protective shell in sp-SERS experiments. For the cases that silica was used as a protective shell, metal nanoparticles were encapsulated in the shells. It was reported that SERS enhancement factors (EFs) for individual Au-SiO<sub>2</sub> core-shell nanoparticles range from  $6.6 \times 10^6$  to  $4.8 \times 10^8$ .<sup>40</sup> Xia and co-workers studied the SERS of 4-mercaptobenzoic acid (4-MBA) adsorbed on silver nanocubes, which were then coated with silica of different thickness.<sup>41</sup> The effect of silica shell on the SERS intensity was investigated and the results were consistent with that of theoretical calculations. Unlike coating the probe molecules outside metal nanoshells, Nie *et al.* covered gold nanoparticles with probe molecules, then controlled coupling agent concentrations to coat silica shells.<sup>42</sup> Such core-shell nanoparticles had a built-in mechanism for signal amplification as compared with fluorescent dyes and quantum dots.<sup>42</sup>

Silica is also applied as a core-template in several sp-SERS studies. Gold nanoshells with a 200 nm SiO<sub>2</sub> core and a 30–40 nm gold layer were reported to be used in flow spectroscopy with a high spectral resolution for rapid SERS detection.<sup>43</sup> When this SiO<sub>2</sub>-Au core-shell nanoshell adsorbed a monolayer of 4-MBA, a nanoscale pH meter could be obtained because the SERS spectra of 4-MBA on nanoshells were very sensitive to the environments with various pH values.<sup>44</sup> Similarly, Emory *et al.* reported another pH-probe by using silica-gold core-shell nanoparticles adsorbing 4-mercaptopyridine (4-MPy). These individual silica-gold core-shell nanoparticles also demonstrated more reliable SERS spectra compared to aggregates of silica-gold core-shell nanoparticles.<sup>45</sup>

## 2.2 One-dimensional nanomaterials

Typical 1D nanomaterials can be either nanorods (NRs) or nanowires (NWs). SERS study on individual NRs/NWs has received growing interest recently. For example, Kim's group synthesized free-standing single-crystalline Ag NWs *via* a simple vapour phase process for single-nanowire SERS.<sup>46</sup> They found that SERS intensity of the Ag NWs had a strong dependence on laser polarization. Finite difference time domain (FDTD) simulation showed that the electric field

was strongly enhanced when the polarization of the laser was normal to the axis of Ag NWs, which agreed well with the experimental results.<sup>46</sup> Recently, SERS of individual nanowires with bulb humps was investigated by Du *et al.*<sup>47</sup> Strong SERS activity was observed from the position of bulb humps. The effect of laser polarization was also discussed on the SERS activity of Ag NWs with bulb humps.<sup>47</sup>

Nanobars and nanorices are also types of 1D nanomaterial that have been studied in sp-SERS. Xia and co-workers reported the syntheses of silver nanobars and nanorices, and studied the effect of polarization on their sp-SERS.<sup>48</sup> Fig. 4 shows that SERS intensity on a single nanobar illuminated by transversely polarized laser is much greater as compared to that of longitudinally polarized laser. Conversely, SERS intensity from an individual nanorice particle showed different polarization dependence (Fig. 4). The authors believe that such difference can be related to the resonance of laser excitation with the different surface plasmon resonances of these two 1D nanomaterials. Comparing with 0D nanocube, nanobar and nanorice have unique 1D structures and anisotropic SERS responses, which allows a better understanding of the polarization effect on the SERS-active nanomaterials.

Single-wire SERS is not limited to noble metal nanostructures. For example, Krishnadas *et al.* synthesized nickel nanowires using a wet chemistry method and investigated their SERS properties by using crystal violet as a probe molecule.<sup>49</sup> The SERS signal from the nickel nanowire substrates was relatively strong, even down to  $10^{-5}$  M crystal violet concentration.

### 2.3 Two-dimensional nanomaterials

Single-particle SERS substrates can also be 2D nanomaterials which are fabricated by either photolithography or nanolithography. The size and shape of the 2D nanomaterials can be finely controlled, allowing a high reproducibility in the SERS intensity. For example, gold nanobowties were successfully fabricated using an electron-beam lithography method.<sup>50</sup> The nanobowtie consists of two metallic triangles oriented tip to tip, and the gap between them can be controlled to below 20 nm. For such nanostructures, chemical enhancement of the substrates can be estimated since the electromagnetic enhancement of the structure can be experimentally measured. The chemical enhancement from an individual nanobowtie absorbing *p*-mercaptoaniline molecules is reported as large as  $10^7$ .<sup>50</sup>

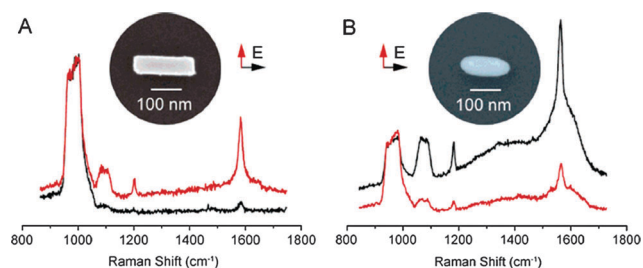


**Fig. 4** SERS spectra from individual nanobar (A) and nanorice (B) covered by a 1,4-benzenedithiol monolayer. Spectra with a transverse laser polarization are shown in red and the longitudinal polarization in black. The spectra were normalized to the silicon band. Reprinted with permission from ref. 48. Copyright 2007, American Chemical Society.

Nanoapertures are also considered as 2D nanomaterials for sp-SERS. Nanoapertures were milled *via* a focused ion beam in optically thick gold film, and fabricated on a gold-coated glass coverslip.<sup>51</sup> The diameters of the apertures can be finely controlled from 100 to 300 nm. It is demonstrated that a SERS EF of  $2 \times 10^5$  can be obtained from an individual gold aperture with a diameter of 100 nm using *p*-mercaptoaniline as the probe molecule. The EF increases when the nanoaperture diameter decreases from 300 to 100 nm. Similarly, Xu *et al.* prepared nanoapertures in gold thin films on silica substrates by a self-assembly colloidal lithography method.<sup>52</sup> The SERS intensities from individual nanoholes in gold film, individual gold particles on a glass, and combined hole-particle systems were compared. Both three-dimensional FDTD simulation and experimental observation revealed that SERS signals from individual nanoholes in a gold film could be much more easily observed.<sup>52</sup>

### 2.4 Three-dimensional nanomaterials

Three-dimensional nanomaterials usually contain complex nanostructures with numerous Raman hot spots inside, which can generate strong SERS signals. Silver stars were synthesized using poly(lactic-*co*-glycolic) acid nanoparticles as templates with a two-step silver reduction method.<sup>53</sup> These silver stars can be applied as both antibacterial agents and SERS substrates. Individual silver stars can be used as an interesting SERS substrate due to the existence of Raman hot spots.<sup>53</sup> Gold nanostars were also reported *via* a one-pot aqueous synthesis.<sup>54</sup> SERS signals from individual gold nanostars could be easily observed without the formation of junctions among aggregated nanostars. It is explained that the SERS signal can be generated from the probe molecules at the tips of the nanostar where the field enhancements have been shown to be the largest.<sup>54</sup> SERS intensities generated from individual gold nanostars have the same order of magnitude as the dimer nanoantennas fabricated by lithography.<sup>54</sup>

It is worth noting that complex nanostructures can also be fabricated *via* physical methods. For example, gold nanobowls were fabricated by Ye and co-workers *via* an ion milling process.<sup>55</sup> Such nanobowls showed a symmetry-reduced geometry and their optical properties were tunable. As shown in Fig. 5, the local electromagnetic field enhancement in the edge position I and center position II on the top of a nanobowl can be significantly different. Based on the FDTD simulation, the SERS intensity at position I can be three to four orders magnitude higher than that of position II. By using carbon nanoparticles as Raman reporters, the authors successfully demonstrated the huge difference for SERS signals at these

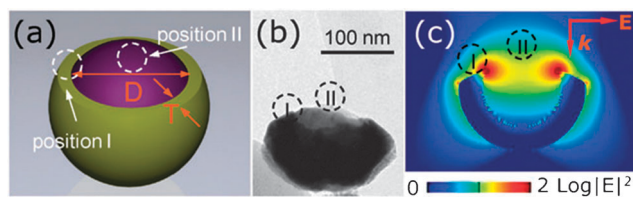


**Fig. 5** (a) Schematic geometry, (b) TEM image and (c) FDTD simulated electric field profile of an Au nanobowl. Reproduced with permission from ref. 55. Copyright 2010, Royal Society of Chemistry.

different locations. Both experimentally and theoretically, the authors demonstrated an excellent example in designing nanoscale architectures to control the locations of the Raman hot spots in a single 3D nanostructure.

### 3. SERS on nano-junctions

Another active subfield in SERS research is to study the strong SERS signals on individual nanoscale junctions, in which two metal nanostructures are located in close proximity and generate Raman hot spots. Unlike sp-SERS, significant SERS enhancement of the nanoscale junctions can be contributed from the strong interactions between the individual nanoscale building blocks in the overall isolated nanostructures. The pioneering work on producing such SERS substrates was from aggregates obtained from aqueous metal colloid dispersions.<sup>56,57</sup> Comparing to isolated nanoparticles, those aggregates can provide stronger SERS signals. However, uncontrolled aggregations and broad compositions led to many challenges to understand the SERS enhancement. Nanoscale junctions, which can be as simple as nanoparticle dimers, have attracted much attention. There are a large number of reports on SERS studies of individual nanojunctions prepared with a variety of methods, such as drop casting,<sup>58–60</sup> molecular bonded dimerization,<sup>61–68</sup> solid phase synthesis,<sup>69</sup> polymer or ligand bridging,<sup>70,71</sup> lithography,<sup>72,73</sup> polymer encapsulation,<sup>39,65,74,75</sup> angle evaporation,<sup>76</sup> layer-by-layer (LBL) assembly,<sup>77–79</sup> galvanic reaction,<sup>80</sup> and vapor-liquid-solid growth. Here, we will classify the nanojunctions into four categories based on the shapes of the joining nanomaterials: nanoparticle–nanoparticle junction, nanoparticle–nanowire junction, nanowire–nanowire junction, and junctions with metal thin films.

#### 3.1 Nanoparticle–nanoparticle junctions

The exploration of SERS on nanoparticle–nanoparticle junctions has generated plenty of experimental data for a better understanding of the SERS mechanism. Several approaches have been used to prepare nanoparticle–nanoparticle junctions. For example, Duyn and co-workers fabricated silver nanoparticle dimers by a simple drop casting approach (Fig. 6a).<sup>59</sup> Although the method is quite easy, it is of low efficiency for SERS study due to the low percentage of dimers in the product. On the other hand, dimer encapsulation method

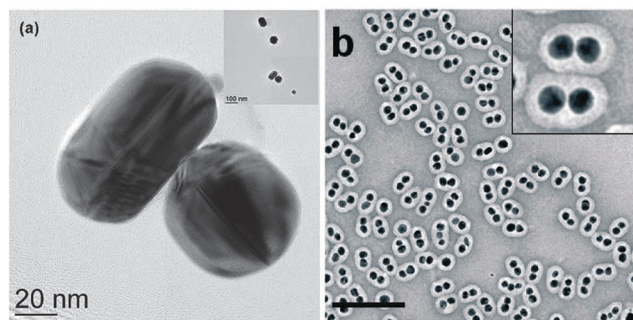
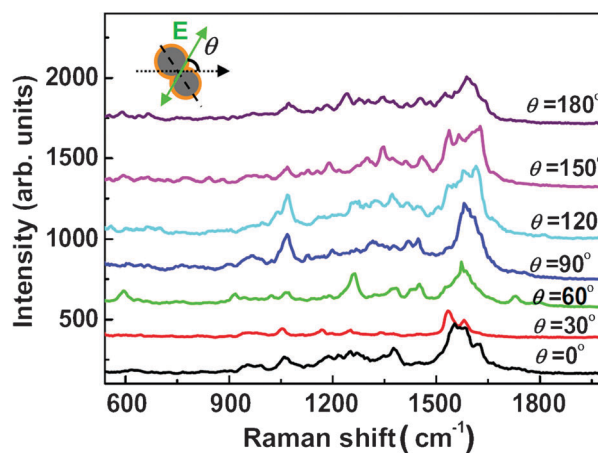


**Fig. 6** (a) Silver nanoparticle dimer fabricated by drop casting; (b) TEM images of Au@Ag dimers. Scale bars: 200 nm. Reprinted with permission from ref. 59 and 74. Copyright 2008 and 2010, American Chemical Society.

can generate nanoparticle dimers with careful experimental designs. Chen's group demonstrated that the majority of their products are pure dimers, as shown in Fig. 6b.<sup>74</sup> The authors have successfully utilized polymer shells to enclose and protect Au@Ag core-shell dimers.<sup>74</sup> This dimerization approach is highly reproducible and the resulting dimers might have a great potential in SERS applications. In another approach, Li and co-workers used cucurbit[*n*]urils (CB[*n*]) to assemble gold nanoparticle–nanoparticle aggregates.<sup>64</sup> In their work, the distance between two connected nanoparticles can be controlled by the size of organic bridged ligands, CB[*n*] molecules.<sup>64</sup> Electrochemically grown heterogeneous Au–Ag–Au nanorods can be used to prepare gold dimers, as demonstrated by Alexander and co-workers.<sup>71</sup> Furthermore, LBL assembly offers a versatile approach to fabricate designed nanoparticle junctions, based on creating multilayered nanoparticles consisting of alternating charged layers.<sup>81–83</sup> For example, Zhang and co-workers reported a novel technique to prepare SERS substrates *via* vertically stacking silver nanodisks, which were separated by a silica layer using the layer-by-layer assembly.<sup>79</sup>

Besides the fabrications of nanoparticle dimers, there are also considerable efforts in studying the polarization-dependent SERS enhancements on these nanoparticle dimers. Chen's group reported an investigation on the relationship between light polarization and SERS activity of silver nanoparticle dimers.<sup>39</sup> As shown in Fig. 7, polarization-dependent SERS activities can be clearly observed on silver nanoparticle dimers. Xia and co-workers developed a plasma etching-based method to study Raman hot spots between two silver nanocubes.<sup>84</sup> In their work, 4-methylbenzenethiol (4-MBT) was used as the SERS probe molecule and a plasma etching process was used to remove the probe molecules outside the hot spots. The much stronger SERS intensities in silver nanocube dimers indicated a higher SERS activity for the dimers than individual nanocubes. In addition, the authors found that the largest SERS enhancement occurred when the laser polarization was parallel to the long axis of the dimers.<sup>84</sup>

Furthermore, Xia's group reported the SERS activities of a variety of well-defined nanoparticle–nanoparticle junctions

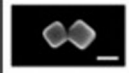


**Fig. 7** Polarization dependent SERS activity of silver nanoparticle dimer with the inset upper left illustration illustrating the angle between the laser polarization direction and the horizontal direction. Reprinted with permission from ref. 39. Copyright 2009, Elsevier.

from two silver nanocubes.<sup>85</sup> In their work, face-to-face, edge-to-face and edge-to-edge structures of two silver nanocubes were randomly assembled by a simple drop-casting method and investigated using both electron microscopy and Raman spectroscopy. The SERS performance of these nano-junctions showed that much higher field-enhancements were obtained from the face-to-face and edge-to-face system, while the lowest field-enhancement was from edge-to-edge ones. They also figured out that the nanoscale sharp features would provide stronger Raman scattering intensities than rounded counterparts, which is consistent with theoretical calculations.<sup>86</sup> In addition, they deduced that higher SERS activity could be achieved when the laser polarization was parallel to the dimer's longitudinal axis. Table 1 provides a summary of the EFs calculated for individual silver nanocubes and three types of dimers under the conditions of perpendicular and parallel laser polarization. Following that, Rabin and co-workers reported another interesting approach to fabricate nanocube dimers in preset locations of patterned substrates.<sup>87</sup> Although the cost is high, their method provided a much better control in fabricating dimer structures than that of the drop-casting method. They showed highest heterogeneity in the SERS intensity with face-to-face dimers while the face-to-edge dimers are more SERS robust. Their work provides valuable information on designing SERS substrates with minimized substrate heterogeneity, which is extremely critical for real sensing applications.

A number of experimental studies on dimer junctions suggest that the SERS enhancement is strongly dependent on the nanoparticle shape, surface roughness and direction of the laser polarization, which is also confirmed by the theoretical calculations. Similar to other numerical simulation packages, FDTD method is highly useful in the study of electromagnetic properties of metallic nanostructures of different geometries.<sup>88–93</sup> For example, Halas and co-workers studied the SERS enhancement from nanoshell and nanosphere dimers.<sup>33</sup> They found that the SERS enhancement from nanoshell dimers was comparable to that of nanosphere dimers when excited by the laser with a parallel polarization.<sup>33</sup>

**Table 1** Summary of the enhancement factors calculated for a single Ag nanocube, and dimers of nanocubes. Arrows in the table correspond to the direction of laser polarization. Reprinted with permission from ref. 85. Copyright 2010 Elsevier

	Enhancement Factor (EF)	
	↔ $7.2 \times 10^5$	↗ $2.5 \times 10^6$
	↔ $2.0 \times 10^7$	↑ $6.6 \times 10^5$
	↔ $1.5 \times 10^7$	↑ $1.9 \times 10^6$
	↔ $5.6 \times 10^6$	↑ $3.0 \times 10^6$

### 3.2 Nanoparticle–nanowire junctions

Another well-defined SERS junction system consists of nanoparticles and nanowires. A variety of fabrication methods has been reported to prepare nanoparticle–nanowire junctions. For example, Kattumenu *et al.* fabricated a SERS active substrate from vertically aligned zinc oxide nanowires, which were uniformly decorated with gold nanorods by a dip coating method.<sup>77</sup> Becker *et al.* made silver nanowires with hemispherical gold droplets on their tip by a vapor–liquid–solid approach.<sup>94</sup> Khan *et al.* reported a method to coat gold islands on GeO<sub>2</sub> nanowires by using an E-beam evaporation.<sup>95</sup> Jiang and co-workers recently reported a LbL approach to fabricate multilayer thin films containing oppositely charged nanorods and nanoparticles, and demonstrated tunable plasmonic properties of the thin films.<sup>78</sup> They also observed enhanced SERS activity from the multilayer thin films, which might offer a feasible method to prepare nanoparticle–nanorod junctions for SERS experiments.

There are several SERS studies on individual nanoparticle–nanowire junctions. Netzer *et al.* reported an intriguing approach in which the nanoparticle–nanowire junctions were formed by a buckling process and studied the SERS intensity map of an individual junction.<sup>96</sup> In their work, an array of aligned silver nanowires was deposited onto a prestrained PDMS substrate and nanobuckles were formed on initially ‘smooth’ silver nanowires after a compressive stress was applied (Fig. 8). This unique nanoscale structure created Raman hot spots in the locations of the junctions between nanobuckles and the nanowire, and enhanced SERS activities were observed at these locations.<sup>96</sup> Tsukruk *et al.* applied polyacrylic acid (PAA) as a linker between silver nanowires and gold nanoparticles to fabricate pH-triggered SERS substrates.<sup>97</sup> Due to the pH sensitivity of PAA, the nanogap between the silver nanowire and gold nanoparticle can be controlled *via* pH adjustment. A wet assembly technique was also used by the same group to fabricate a gold nanoparticle–silver

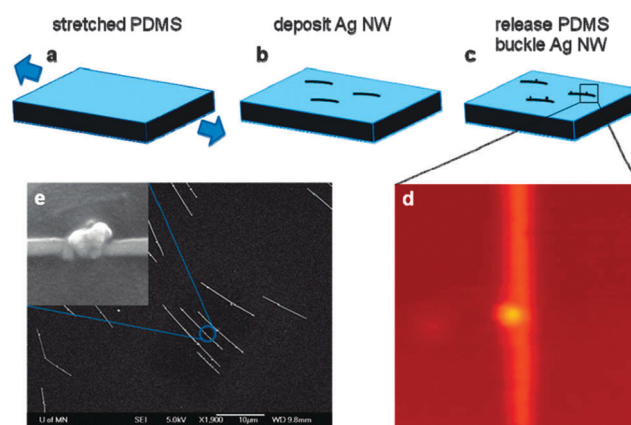


**Fig. 8** Schematics and images of silver nanobuckles: (a–c) compression-induced silver nanobuckle formation by depositing silver nanowires onto a prestrained PDMS substrate; (d) AFM image of silver nanobuckle formed on a silver nanowire (image size:  $5 \times 5 \mu\text{m}^2$ ); (e) SEM micrograph of silver nanobuckles along the silver nanowires. (Inset) A higher magnification ( $25\,000\times$ ), side view (tilt angle,  $30^\circ$ ) SEM micrograph. Reprinted with permission from ref. 96. Copyright 2010, American Chemical Society.

nanowire junction system.<sup>98</sup> Another interesting approach to make nanoparticle–nanowire junctions was reported by Brejna *et al.* where they used a galvanic replacement reaction to produce silver nanoparticles and an Ostwald ripening process was utilized for particle growth.<sup>80</sup> They investigated the SERS activity in the regions where silver nanoparticles were grown. As a result, the SERS enhancements obtained in these regions were at least five times higher than of the particles that did not undergo the ripening process.

Furthermore, geometry effects of nanoparticle–nanowire junction and laser polarization on SERS enhancements have received a lot of interest from researchers.<sup>99–101</sup> Xu and co-workers observed significant SERS enhancement when the incident light was polarized across the junctions of gold nanoparticles and nanowires.<sup>99</sup> Xia and co-workers published an article on the polarization dependent SERS activity at junctions between a silver nanocube and a silver nanowire with sharp corners.<sup>58</sup> Two distinct junction geometries have been investigated: (1) a sharp silver nanocube with one side nearby the silver nanowire (face-to-face); (2) a sharp silver nanocube edge nearby the silver nanowire (edge-to-face). The measurements of EF for single nanocube, single nanowire and the junction systems were compared. They concluded that the largest field enhancement and SERS intensity were obtained when laser polarization was parallel to the long axis of junctions.<sup>58</sup>

### 3.3 Nanowire–nanowire junctions

SERS study on individual junctions of crossing nanowires has received great attention because of the generation of Raman hot spots at the junction region. Several methods were reported on the assembly of nanowire–nanowire junctions and their applications for SERS substrates have been demonstrated.<sup>91,101–103</sup> Moreover, the relationship between laser polarization and SERS enhancement was also investigated.<sup>91,104</sup>

Kang *et al.* reported the construction of crossed or parallel nanowire pairs using a nanomanipulator.<sup>91</sup> In these nanowire pair systems, the intense SERS enhancements observed at the junction directly visualized the existence of the Raman hot spots. The results are fully consistent with the FDTD calculation for the specific nanowire geometries.<sup>91</sup> Glembocki *et al.* reported that the dielectric substrate for crossed nanowires played a critical role in SERS enhancement, according to both experimental results and theoretical calculations.<sup>104</sup> The calculation results of the SERS enhancement for a pair of crossed nanowires at an angle of 45° in air and on a silicon substrate were compared. It is clear that the silicon substrate has an influence on the local electric fields near the contact point.<sup>104</sup> A comprehensive study on wire–wire junctions was done by Chang and co-workers where they used a double-step transversal capillary transfer microprinting approach to fabricate silver nanowire crossbars partially decorated with silver nanoparticles.<sup>101</sup> Different on/off SERS activity on the nanowire–nanowire junction can be designed using a variety of different polarization directions or orientation directions.<sup>101</sup> Yoon *et al.* used an array platform and studied the correlation between the junction conduction properties and molecular structure by SERS on the same junction.<sup>103</sup> Furthermore, Tsukruk's group designed novel hybrid bimetallic silver–gold

core–double–shell nanowires which demonstrated great efficiency of SERS activities.<sup>75</sup> They observed that the SERS enhancements at the individual bimetallic nanowire–nanowire junctions were many times higher than those from silver nanowire junctions.

### 3.4 Junctions on metal thin films

SERS on individual nano-junctions can also be observed when nanoparticles or nanowires interact with an underneath metal thin film so that nanoparticle–thin film junctions or nanowire–thin film junctions were formed. Besides the experimental explorations, there are also active theoretical studies for such type of nano-junctions. For example, Wu *et al.* demonstrated the plasmonic interaction between a nanoshell and adjacent dielectric substrate using FDTD method.<sup>92</sup> Nordlander and co-workers reported the study of surface plasmon interaction in the gold nanoparticle–thin film junctions and nanoshell–thin film junctions by an electromagnetic analogue of the spinless Anderson–Fano model.<sup>105,106</sup>

Several experimental approaches have been developed to study the SERS activity on junctions created by nanoparticles or nanowires with metal thin films.<sup>66,107</sup> Early works in this field started from the favourable effects of metal island films for SERS activity study.<sup>108–111</sup> Ferrell and co-workers produced spheroidal-shaped particles through an annealing process which created a nanoparticle–thin film junction system.<sup>112</sup> Smith *et al.* reported controllable nanoparticle–metal film separation and used a polymer layer to tune the distance between the nanoparticles and metal thin films.<sup>113</sup> Hu *et al.* investigated a system of single silver nanoparticle on a gold film and found that by controlling the thickness of a thin silica spacer layer between the metal nanoparticle and the metal film, an optimum thermally stable substrate could be obtained with superior SERS performance.<sup>114</sup> Zubarev's group synthesized a novel type of starfruit-shaped gold nanorods by using a seed-mediated method. They observed strong SERS signals from individual mesorods deposited on benzenedithiol-coated gold film, which can be closely related to the roughened surface of the gold mesorods.<sup>115</sup>

One interesting study about junctions on metal thin film was reported by Xia and co-workers, who demonstrated that the nanogap between nanoparticles and metal thin film can be well controlled by the thickness of a SiO<sub>2</sub> shell surrounding the nanoparticles.<sup>41</sup> In their work, a silver nanocube was first adsorbed with 4-MBA, then coated with silica shells of different thickness. They observed different SERS intensities on various substrates including gold, silicon and glass, indicating a strong effect of SERS intensity on the type of supporting substrates (Fig. 9). When a glass substrate was used, the SERS intensity of the core–shell nanoparticle did not change much as a function of silica thickness. However, when a gold film was used, the SERS intensity decreased significantly as the thickness of SiO<sub>2</sub> increased. Their results allow a better understanding in the formation of the Raman hot spots between a silver nanocube and its supporting substrate. Similarly, Mangeney and co-workers designed a SERS substrate in which gold nanoparticles were assembled on a gold film surface functionalized with linker molecules.<sup>116</sup> The authors

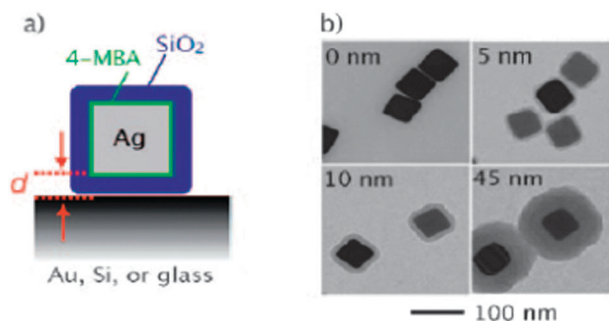


**Fig. 9** (a) Schematic showing how the gap distance  $d$  between a Ag nanocube and its underlying substrate is controlled by the thickness of the SiO<sub>2</sub> shell (blue). The nanocube was functionalized with SERS-active 4-MBA (green) prior to coating with SiO<sub>2</sub>. (b) TEM images of Ag nanocubes coated with SiO<sub>2</sub> shells of thickness 0, 5, 10 and 45 nm, respectively. Reprinted with permission from ref. 41. Copyright 2011, John Wiley and Sons.

were able to tune the SERS ability on and off by changing the substrate temperature which led to the length change of the linker molecules.

Kim and co-workers used a drop casting method to generate a single nanowire on thin film platform (SNOF), from which a Raman signal was obtained at a level suitable for a practical biosensor.<sup>93</sup> This SNOF structure provided a line of Raman hot spots at the gap between the nanowire and the film, which can be conveniently located *in situ* using an optical microscope. Fig. 10 shows SERS spectra of brilliant cresyl blue (BCB), benzenethiol (BT) and a thiolated 10-mer adenine ssDNA (HS-A<sub>10</sub>) adsorbed onto gold nanowire–gold thin film structures and gold nanowires–silicon substrates. SERS signals were observed from the SNOF systems for all three molecules. And they are much stronger for the Au/Au SNOF system as compared with gold nanowire on a silicon substrate.

#### 4. SERS on aggregation

Besides individual nanoparticulates and nano-junctions, more complicated nanostructures (and aggregations) have been developed in SERS study and these hierarchical nanostructured

materials present excellent SERS performance with robust intensity, excellent reproducibility, and low detection limits. In the following, we will discuss some unique 3D hierarchical nanostructures and the SERS performances on these individual structures.

#### 4.1 Nano-aggregation

Aggregated nanostructures have been well developed and widely applied into SERS detections since the gathered nanoparticles can largely enhance local plasmon resonance, which can result in impressive SERS abilities. Silver colloidal particles and gold nanoparticle aggregates have been employed as highly active SERS substrates.<sup>93,117,118</sup> Cao's group successfully controlled colloidal superparticle growth through solvophobic interactions and their colloidal superparticles made of gold nanoparticles exhibited strong SERS signals upon doping with R6G, which can be due to the electromagnetic field enhancement from the gold superparticles.<sup>119</sup> Zhang's group developed SERS-active substrates containing gold nanoparticle aggregates and an EF up to 10<sup>7</sup> was reported for R6G Raman signals.<sup>117</sup> Singamaneni and co-workers assembled core–satellite gold nanostructures using simple molecular cross-linkers and obtained strong SERS activities due to the in-built Raman hot spots.<sup>120</sup> In another example, SERS properties of thiocarbocyanine J- and H-aggregates adsorbed on individual silver aggregates have been investigated by Kitahama *et al.* and single osteosarcoma cells can be studied in detail using colloidal gold nanoparticles as substrate in near-infrared SERS detection.<sup>121,122</sup>

It is noteworthy that well arranged nano-aggregates have also been developed as SERS-active substrates. Jiang and co-workers fabricated freestanding LbL thin films with embedded gold nanorod arrays.<sup>123,124</sup> Recently, a wrinkle confined gold nanoparticle substrate was fabricated and its SERS activities were investigated by Liz-Marzán's group.<sup>125</sup> The gold nanoparticle arrays were originated using a pre-stretched PDMS substrate (Fig. 11). Those arrays can be tuned to create single and double lines of gold nanoparticles. These gold nanoparticle arrays showed high SERS ability and extremely uniform SERS enhancement.<sup>125</sup> The method used

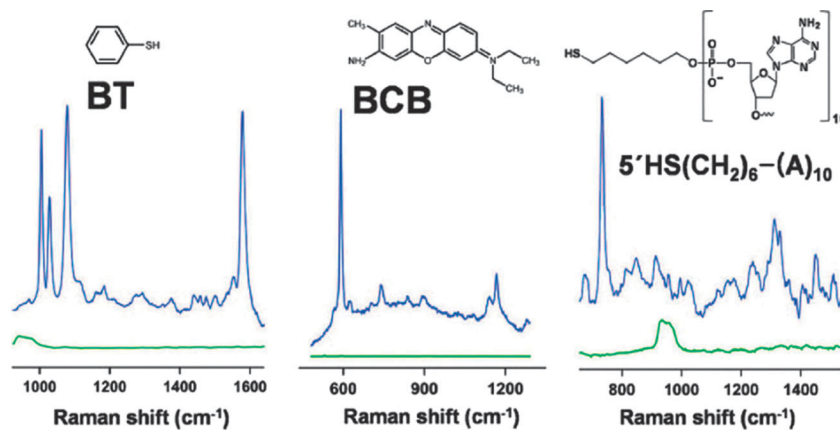


**Fig. 10** SERS spectra of BT, BCB and HS-A<sub>10</sub> for (blue) the Au/Au SNOF system and (green) a Au NW on a Si substrate. The peak near 850 cm<sup>-1</sup> in the green trace is a Si Raman peak. The polarization of the incident light is perpendicular to the NW axis. Reprinted with permission from ref. 93. Copyright 2010, American Chemical Society.

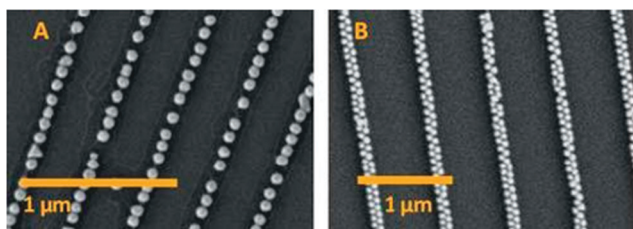


**Fig. 11** SEM images of single and double line aligned Au nanoparticles. Reprinted with permission from ref. 125. Copyright 2010 Royal Society of Chemistry.

for fabricating gold nanoparticle arrays is very simple, efficient and cost effective. However, such approach is hard to be industrialized.

While the aggregated silver or gold nanoparticles can be utilized in SERS detection, a combination of nanomaterials and biomaterials with precisely controlled aggregated gaps can result in high SERS uniformity and enormous enhancement. Recently, Lim *et al.* reported highly-uniform gold nanoparticles with 1 nm interior gap prepared using a DNA-tailored method.<sup>126</sup> Those SERS active nanostructures, denoted gold nanobridged nanogap particles, displayed Raman signals with ultra-high enhancement, reproducibility and uniformity. The interior hollow gap (about 1 nm) between the gold core and shell can be precisely manipulated by tailoring DNA molecules in between gold nanoparticles.<sup>126</sup>

As shown in Fig. 12, TEM images illustrated different stages of DNA modified gold nanobridged nanogap particle formation, from side modified Au–DNA particles to half-shell covered Au–DNA particles.<sup>126</sup> TEM results also showed well-defined gaps in the uniform gold nanobridged nanogap particles. Detailed morphology of a single gold nanobridged nanogap particle is shown in the HRTEM image and the element mapping analysis of the crossing line, from which a 1.2 nm interior nanogap is clearly demonstrated. The precise

control of the nanoscale gaps can largely magnify the SERS enhancement which was demonstrated in both experimental results and theoretical calculations.<sup>126</sup> From Raman mapping analysis, the authors found that SERS signals generated from these gold nanoparticle aggregate substrates were highly sensitive with a probe concentration down to 10 fM and the SERS EF was up to  $10^8$  for more than 90% area.<sup>126</sup>

## 4.2 Nanowire-based hierarchical nanostructures

Nanowires have attracted enormous interests due to their unique 1D structures and electrical, optical, mechanical and thermal properties. Nowadays, nanowires are not only widely studied in various fields as typical 1D building blocks for functional materials, but also employed as templates to fabricate hierarchical nanostructures for SERS and other applications. For example, Qi *et al.* reported the deposition of silver nanoparticles on the surface of zinc oxide nanowires, and strong SERS signals were observed.<sup>127</sup> Fang and co-workers grew silver nanoparticles on silicon nanowires and successfully observed single-wire SERS enhancement.<sup>128</sup> They also demonstrated that their method was suitable for preparing large-scale SERS-active silver–silicon nanowire arrays. Singamaneni's group used aligned electrospun nanofibers as templates to assemble gold nanorods and observed orientation-dependent SERS intensity on individual anisotropic nanofibers.<sup>129</sup>

Recently, Jiang and co-workers manufactured bimetallic gold–silver nanowires *via* a simple galvanic replacement reaction and observed a dramatically increased SERS enhancement on individual nanowires.<sup>130</sup> To prepare the bimetallic nanowires, the pristine silver nanowires were treated with HAuCl<sub>4</sub> solution, and then rinsed by DI water. This process generated bimetallic nanowires with numerous nanoparticles and porous structures. The porous features were further identified by a combination of electron microscopy and spectroscopy. Due to the high porosity of nanostructures,

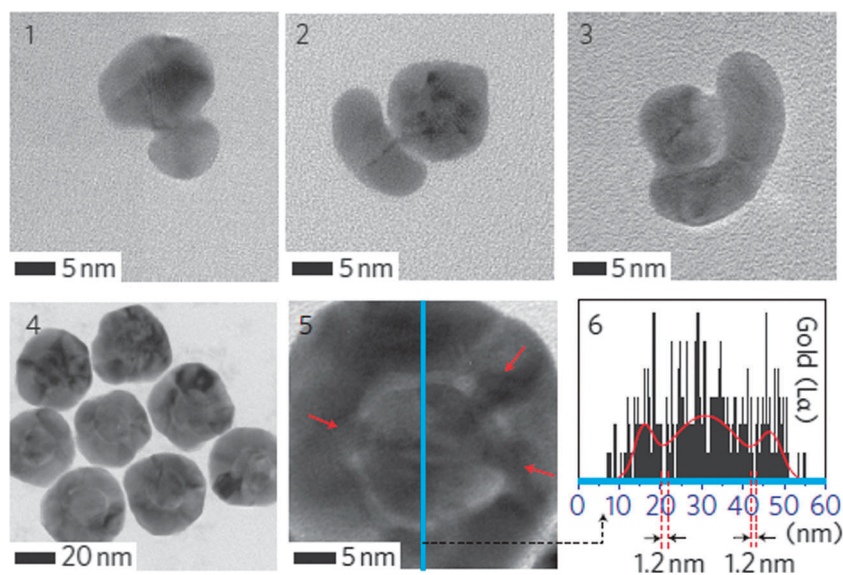


**Fig. 12** TEM images show the formation of Au nanobridged nanogap particles (1–4) and morphologies. The nanobridges are revealed in panel 5, and panel 6 represents the element line across a particle (panel 5 blue line). Reprinted with permission from ref. 126. Copyright 2011, Nature Publishing Group.

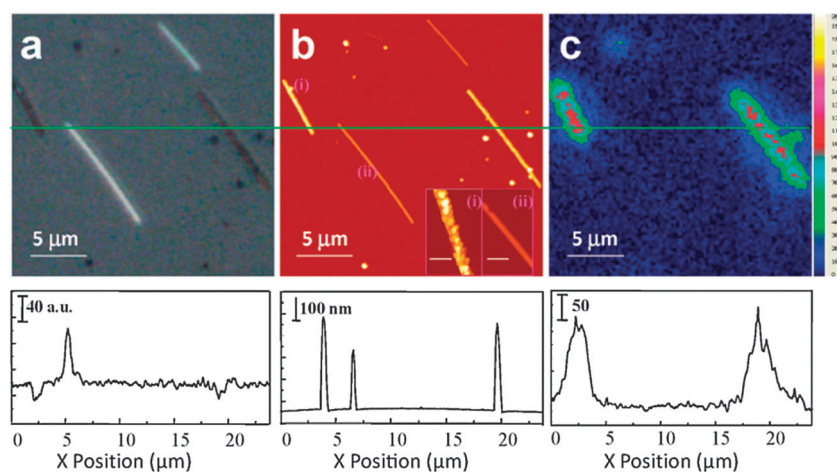


**Fig. 13** Optical, AFM images (a, b), and Raman map (c) in the same scanning location. Insets: enlarged AFM images. The line scan of both silver nanowires and bimetallic gold–silver nanowires in the region of interest are shown below.

those bimetallic nanowires showed excellent SERS ability when compared to pristine silver nanowires.<sup>130</sup>

Comparison of gold–silver bimetallic nanowires with pristine silver nanowires is shown in Fig. 13. The three panels represent the optical image, atomic force microscopic (AFM) image, and Raman map for the nanowires in the same area, respectively. The optical image clearly indicated that pristine silver nanowires are more reflective compared to the bimetallic nanowires. This can be explained by that after galvanic replacement, highly porous Au–Ag nanowires were formed which resulted in more scattered light than direct reflectance. This phenomenon can be used to optically distinguish the bimetallic nanowires and pristine ones. The AFM images reveal the rough surface of the bimetallic nanowires, which could enhance adsorption capability and adsorb more probe molecules than that of the pristine ones. The Raman map shows impressive SERS enhancement on the bimetallic nanowires compared to pristine nanowires. Strong SERS enhancement can be clearly observed on two individual bimetallic nanowires, while there are almost no Raman signals on the two pristine silver nanowires. This result clearly indicates that surface modification is an easy and effective option to fabricate SERS-active hierarchical nanostructures.<sup>130</sup>

On-wire lithography, an emerging technique which has been used in nano-scale engineering, has also been employed to fabricate nanorings. Such engineered nanostructures have demonstrated excellent SERS performance, from both individual nanorings and nanoring-based arrays. Liusman *et al.* reported a new approach to fabricate free-standing bimetallic nanorings and nanoring arrays using a combination of on-wire lithography and galvanic replacement reaction.<sup>131</sup> The aspect ratio of the nanorings can be tuned and the nanorings arrays can be produced with desired numbers of nanorings and spacing in between. Fig. 14 shows the morphology evolution of the hierarchical nanorings. The striped Ag–Ni nanowire structure was synthesized *via* an electrochemical deposition. After galvanic replacement reaction with boiling HAuCl<sub>4</sub> solution, the nickel segment can be completely released by aqueous HCl etching, leaving bare bimetallic nanorings. Although the fabrication process was complicated, expensive

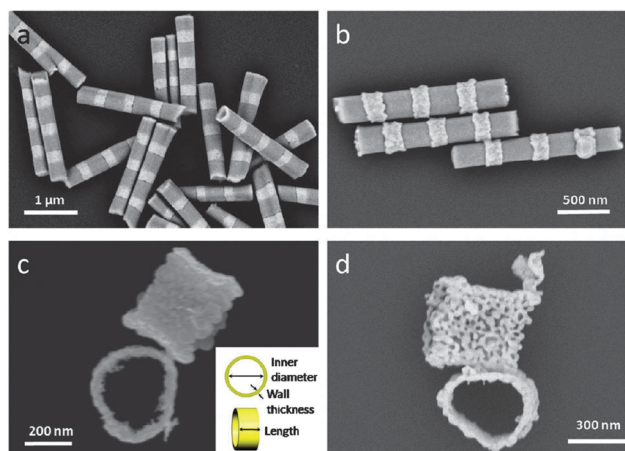


**Fig. 14** SEM images of Ag–Ni nanorods fabricated by electrochemical deposition. (a, b) Ag–Ni nanorods after galvanic reaction, (c) bimetallic nanorings and (d) post-etched porous nanorings. Reprinted with permission from ref. 131. Copyright 2010, American Chemical Society.

and quite time consuming, these nanorings and their arrays exhibited excellent SERS property in both experimental results and theoretical calculations.<sup>131</sup>

### 4.3 3D hierarchical nanostructures

It has been realized that controllable hierarchical nanostructures might provide SERS-active substrates with superior SERS performance. Shape evolved study on three-dimensional, hierarchical nanostructures have attracted enormous interests. Through the evolution of 3D hierarchical nanostructure, we can have a better understanding of Raman hot spots and so aid optimization

A typical 3D hierarchical nanostructure is the so-called nanoflower or nanomeatball. There are two merits of those nanostructures for their usage in SERS applications: (1) larger surface area to adsorb probe molecules on the surface, compared to regular shapes and smooth surface nanoparticles; (2) nanoscale features on their surface, which potentially provide more opportunity to create Raman hot spots even in

individual nanoflowers or nanomeatballs. Two approaches were used to prepare those 3D hierarchical nanostructures: direct synthesis and post-synthesis chemical treatment.<sup>132,133</sup> For instance, Xu and co-workers used a one-pot synthesis method and prepared gold nanoflowers.<sup>134</sup> A facile polyol method was then developed to synthesize gold nanoflowers with highly branched structure using amine-reducing agents.<sup>135</sup> The SERS performance of the gold nanoflowers was investigated by using 4-MPy as probe molecules.<sup>135</sup> Due to the nanoscale roughness on the surface of nanomeatball or nanoflower, those 3D hierarchical structures demonstrated excellent SERS enhancement and raised their profiles in SERS applications.

Wang and co-workers synthesized gold meatball particles, and studied their optical properties and SERS applications (Fig. 15).<sup>136</sup> Surface roughened flower shape silver nanoparticles were also fabricated and those particles exhibited high sensitivity in SERS tests.<sup>137</sup> In this report, the single particle polarization dependent-SERS properties were cautiously identified.<sup>137</sup> Xie and co-workers developed a one-pot approach to synthesize gold nano-branched nanoparticles at room temperature.<sup>138</sup> There are more than ten tips on a single gold nanoparticle surface which shows exceptional SERS ability. Those gold nanoparticles showed good size monodispersity which can be applied as tags for *in vivo* applications.<sup>138</sup> More recently, a facile particle-mediated aggregation method was used to synthesize gold mesoparticles.<sup>132</sup> The authors prepared the mesoparticles using FeCl<sub>3</sub> solution to reduce HAuCl<sub>4</sub> aqueous solution with different reaction times. Those mesoparticles with tunable surface morphology can be self-assembled into mono- or multi-layer particle arrays with a high uniformity. The authors reported a high SERS enhancement on individual gold mesoparticles. Furthermore, they observed a further one or two orders of magnitude improvement for mesoparticle arrays due to additional Raman hot spot formation between the mesoparticles.

Employing templates to build gold or silver based nanocages is another route to synthesize mesoparticles. Cu<sub>2</sub>O particles with morphology variation from spherical, cubic to octahedral were utilized as templates to react with HAuCl<sub>4</sub> solutions. By using this method, Fang and co-workers fabricated

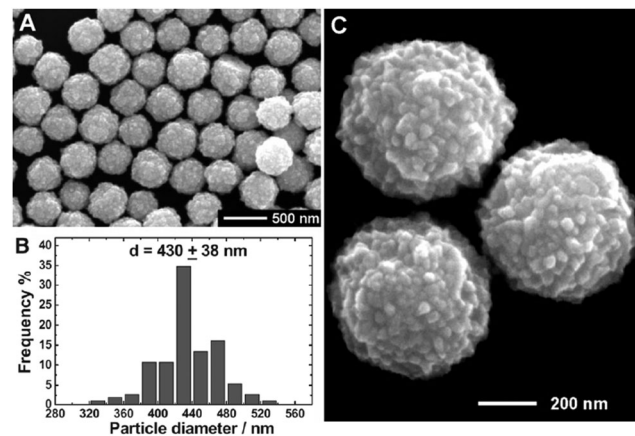


**Fig. 15** SEM images of meatball structures and their size distribution. Reprinted with permission from ref. 136. Copyright 2008, John Wiley and Sons.

polyhedral gold mesocages with highly roughened surface, including numerous effective hot spots, which can lead to a substantial contribution to SERS performance.<sup>133</sup> The shape-dependent SERS activities were also investigated. Single-particle SERS spectra and Raman maps of crystal violet were investigated on gold mesocages with different morphologies: (a) mesocage, (b) spherical, (c) cubic and (d) octahedral. The method is highly repeatable and the products have demonstrated remarkable SERS activity with EF up to  $10^7$ – $10^8$ . A similar route for silver mesocage fabrication was also investigated by the same group.<sup>139</sup>

Besides nanoflowers and nanocages, other types of 3D hierarchical nanostructures were also fabricated directly and their SERS activities were examined. For example, Roeffaers and co-workers fabricated silver dendritic nanostructures *via* a photocatalytic growth.<sup>140</sup> Typically, dendritic nanostructure was grown from a silver nitrate solution in the presence of ZnO crystals under UV light irradiation. With a large amount

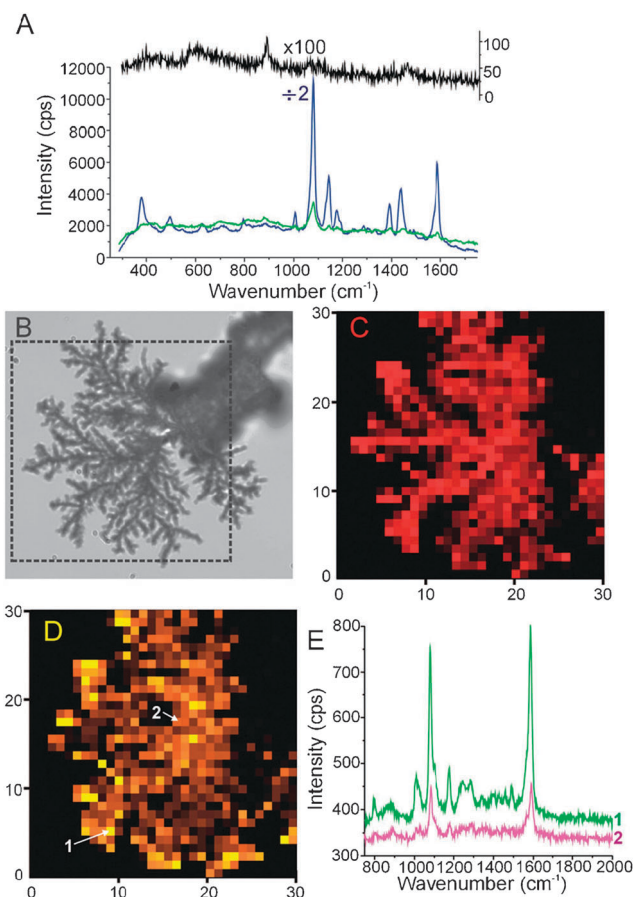


**Fig. 16** Dendritic silver nanostructures as SERS substrates: (A) comparison of the Raman spectra of an ethanolic solution containing 4-MOTP recorded in the presence (blue, green) and absence (black) of the SERS substrate; the concentration of 4-MOTP is 100 nM (green), 1 mM (blue) and 100 mM (black). (B)–(D) Micrographs of dendritic silver structures submerged in an ethanolic 4-MOTP solution: (B) optical transmission image, (C) photoluminescence image (650–750 nm) and (D) Raman map (1060–1120 cm<sup>-1</sup>). (E) Two representative SERS spectra extracted from the Raman map (D) at positions 1 and 2. Reprinted with permission from ref. 140. Copyright 2012, Royal Society of Chemistry.

of nanoscale features contributing as Raman hot spots, these dendritic nanostructures exhibited remarkable SERS enhancement at low detectable concentration using 4-methoxythiophenol as a probe molecule. Fig. 16 shows the optical transmission image and the Raman map, from which the authors demonstrated that large dendritic silver nanostructures possess excellent SERS ability. One drawback of this dendritic structure is that the Raman hot spots are not uniformly distributed, as shown in the Raman map. The Raman bands of the probe molecules indicated in positions 1 and 2 are quite different in intensity and further optimization in substrate preparations is required for any practical applications. Another SERS-active nanostructure, gold nanoleaves, were synthesized using 2-thiophenemethanol to reduce HAuCl<sub>4</sub> solution at room temperature.<sup>141</sup> Since this structure enriches the nanoscale gaps, it showed high performance in SERS application for several molecules such as methyl blue and crystal violet.<sup>141</sup>

## 5. Applications and outlook

The extremely active sp-SERS studies on isolated nanostructures have provided an excellent opportunity in designing novel SERS-active substrates with superior performance. Furthermore, these individual nanostructures, including nanoparticulates, nanoscale-junctions, and nano-aggregates, have demonstrated great potential as unique sensing materials for a variety of applications, such as environmental monitoring, pH sensing, biomaterials sensors, ultralow trace chemical detection, and food safety, to name a few.

### 5.1 Design of novel SERS-active nanomaterials

One of the most important applications for single-particle SERS study is to enable designs of novel nanostructures for unprecedented functionality and performance, based on a better understanding of structure–property relationship at the single-particle level. For example, Yang *et al.* synthesized complex nanoparticles with highly anisotropic shapes by controlling the etching kinetics. These silver nanostructures showed tunable localized surface plasmon peaks across the spectra of visible and near IR, and possessed highly sp-SERS sensitivities. Their detailed study on the structure–property relationship allows a further design of multiplex sensing materials for detecting multiple analytes.<sup>31</sup> Similarly, Willets and co-workers mapped the position of single-molecule SERS with a 10 nm resolution on isolated nanoparticles and their assemblies.<sup>23,31</sup> Their work demonstrated a unique approach in identifying the locations of the Raman hot spots within a single diffraction-limited spot, thus providing valuable information in designing SERS-active nanostructures.

### 5.2 sp-SERS based sensing and imaging

Single-particle SERS has demonstrated great potentials in various sensing and imaging applications, such as pH sensing, monitoring of heavy metals in water, and biomolecular imaging. There have been several reports on developing pH sensing substrates based on the single-particle SERS technique. Talley and co-workers demonstrated the suitability of using 30 nm hollow gold nanoparticles for pH sensing.<sup>32</sup> The authors believe that the sensitivity of the pH probe is due to the strong

SERS enhancement of individual hollow nanoparticles.<sup>32</sup> Similarly, a nanoscale pH meter was reported by Halas and co-workers using gold nanoshells and an average accuracy of 0.10 pH units across its operating range was achieved. Single-particle SERS was also applied for trace metal ion detection. For example, Chung's group designed a mercury sensor using DNA-modified gold microshells. The authors obtained a detection limit of 50 nM for sensitive and selective mercury(II) ion detection *via* a small volume analysis.<sup>142</sup> One example of preparing an excellent SERS probe for single-particle biomolecular imaging was shown by Lee and co-workers.<sup>143</sup> The authors applied biocompatible magnetic nanocrescents as controllable SERS probes and demonstrated an EF higher than 10<sup>8</sup> in detecting sub-zeptomole molecular concentrations. Their work allows further biofunctionalization on these highly SERS active nanostructures for real-time biomolecular imaging.<sup>143</sup>

### 5.3 sp-SERS based spectroscopic tags in liquid flow

sp-SERS has been utilized as nanoscale spectroscopic tags in liquid flow systems and so providing an efficient approach for *in situ* quality control in continuous processes. Methods of high-throughput flow-based platform for SERS detections have been developed. For example, Laurence *et al.* described an efficient and rapid method toward high-throughput detection using fluorescence and Raman correlation spectroscopies to investigate solution-based SERS intensity through a confocal laser spectrometer.<sup>34</sup> Later, Goddard *et al.* demonstrated an efficient method of individual nanoparticle SERS detection in flow systems.<sup>144</sup> They used a full spectral Raman flow cytometer to rapidly investigate SERS intensity variations among nanoparticle populations. Similarly, Cecchini and co-workers detected single nanoparticles using a combination of correlation spectroscopy and surface-enhanced resonance Raman spectroscopy.<sup>145</sup> They used gold nanoparticles labelled with reporter molecules on a custom-built Raman spectrometer and deduced that measurements based on liquid flow allowed for a higher throughput of detected events with shorter analysis times.

### 5.4 sp-SERS outlook

Significant progress has been made in designing, fabricating and understanding individual nanostructures with high SERS activities. Future research efforts are expected in following areas: (1) further improvement of the SERS enhancement from individual nano-objects *via* nanoscale control of the materials and structures; (2) better understanding of the Raman hot spots with novel experiments, such as *in situ* study of structure–property relationship on individual nano-objects; (3) improved simulations of the Raman hot spots with theoretical approaches; (4) optimization and integration of SERS-active nano-objects for molecular and biomolecular identifications. All these will open up additional opportunities for fabricating new-generation SERS-active substrates with giant enhancement and superior sensing capability, which can dramatically expand the applications of SERS to even broader fields.

## Acknowledgements

The authors would like to thank support from the National Science Foundation/EPSCoR Grant No. 0903804, from the NASA (Cooperative Agreement Number: NNX10AN34A) and from the State of South Dakota.

## Notes and references

- J. A. McMahon, Y. M. Wang, L. J. Sherry, R. P. Van Duyne, L. D. Marks, S. K. Gray and G. C. Schatz, *J. Phys. Chem. C*, 2009, **113**, 2731–2735.
- J. Zhang, Y. Fu, M. H. Chowdhury and J. R. Lakowicz, *Nano Lett.*, 2007, **7**, 2101–2107.
- M. Hu, C. Novo, A. Funston, H. N. Wang, H. Staleva, S. L. Zou, P. Mulvaney, Y. N. Xia and G. V. Hartland, *J. Mater. Chem.*, 2008, **18**, 1949–1960.
- L. H. Guo and D. H. Kim, *Chem. Commun.*, 2011, **47**, 7125–7127.
- S. Schietinger, T. Aichele, H. Q. Wang, T. Nann and O. Benson, *Nano Lett.*, 2010, **10**, 134–138.
- C. L. Du, Y. M. You, J. Kasim, Z. H. Ni, T. Yu, C. P. Wong, H. M. Fan and Z. X. Shen, *Opt. Commun.*, 2008, **281**, 5360–5363.
- M. S. Dresselhaus, A. Jorio and R. Saito, *Annu. Rev. Condens. Matter Phys.*, 2010, **1**, 89–108.
- C. Y. Jiang, J. L. Zhao, H. A. Therese, M. Friedrich and A. Mews, *J. Phys. Chem. B*, 2003, **107**, 8742–8745.
- C. Y. Jiang, J. X. Li, J. L. Zhao, U. Kolb and A. Mews, *Nano Lett.*, 2002, **2**, 1209–1213.
- L. Polavarapu, K. K. Manga, K. Yu, P. K. Ang, H. D. Cao, J. Balapanuru, K. P. Loh and Q. H. Xu, *Nanoscale*, 2011, **3**, 2268–2274.
- K. C. Bantz, A. F. Meyer, N. J. Wittenberg, H. Im, O. Kurtulus, S. H. Lee, N. C. Lindquist, S. H. Oh and C. L. Haynes, *Phys. Chem. Chem. Phys.*, 2011, **13**, 11551–11567.
- N. Tarcea, T. Frosch, P. Rosch, M. Hilchenbach, T. Stuffer, S. Hofer, H. Thiele, R. Hochleitner and J. Popp, *Space Sci. Rev.*, 2007, **135**, 281–292.
- J. A. Dieringer, K. L. Wustholz, D. J. Masiello, J. P. Camden, S. L. Kleinman, G. C. Schatz and R. P. Van Duyne, *J. Am. Chem. Soc.*, 2009, **131**, 849–854.
- J. R. Lombardi and R. L. Birke, *J. Phys. Chem. C*, 2008, **112**, 5605–5617.
- J. R. Lombardi and R. L. Birke, *Acc. Chem. Res.*, 2009, **42**, 734–742.
- L. D. Qin, S. L. Zou, C. Xue, A. Atkinson, G. C. Schatz and C. A. Mirkin, *Proc. Natl. Acad. Sci. U. S. A.*, 2006, **103**, 13300–13303.
- S. M. Nie and S. R. Emery, *Science*, 1997, **275**, 1102–1106.
- S. R. Emory, R. A. Jensen, T. Wenda, M. Y. Han and S. M. Nie, *Faraday Discuss.*, 2006, **132**, 249–259.
- J. T. Krug, G. D. Wang, E. Sr and S. M. Nie, *J. Am. Chem. Soc.*, 1999, **121**, 9208–9214.
- W. E. Doering and S. M. Nie, *J. Phys. Chem. B*, 2002, **106**, 311–317.
- E. Sr and S. M. Nie, *Anal. Chem.*, 1997, **69**, 2631–2635.
- A. M. Michaels, M. Nirmal and L. E. Brus, *J. Am. Chem. Soc.*, 1999, **121**, 9932–9939.
- S. M. Stranahan and K. A. Willets, *Nano Lett.*, 2010, **10**, 3777–3784.
- J. Kneipp, H. Kneipp and K. Kneipp, *Chem. Soc. Rev.*, 2008, **37**, 1052–1060.
- N. P. W. Pieczonka and R. F. Aroca, *Chem. Soc. Rev.*, 2008, **37**, 946–954.
- X. M. Qian and S. M. Nie, *Chem. Soc. Rev.*, 2008, **37**, 912–920.
- S. Buchanan, E. C. Le Ru and P. G. Etchegoin, *Phys. Chem. Chem. Phys.*, 2009, **11**, 7406–7411.
- K. L. Wustholz, C. L. Brosseau, F. Casadio and R. P. Van Duyne, *Phys. Chem. Chem. Phys.*, 2009, **11**, 7350–7359.
- E. Sr, W. E. Haskins and S. M. Nie, *J. Am. Chem. Soc.*, 1998, **120**, 8009–8010.
- J. M. McLellan, Z. Y. Li, A. R. Siekkinen and Y. N. Xia, *Nano Lett.*, 2007, **7**, 1013–1017.
- M. J. Mulvihill, X. Y. Ling, J. Henzie and P. D. Yang, *J. Am. Chem. Soc.*, 2010, **132**, 268–274.
- A. M. Schwartzberg, T. Y. Oshiro, J. Z. Zhang, T. Huser and C. E. Talley, *Anal. Chem.*, 2006, **78**, 4732–4736.
- C. E. Talley, J. B. Jackson, C. Oubre, N. K. Grady, C. W. Hollars, S. M. Lane, T. R. Huser, P. Nordlander and N. J. Halas, *Nano Lett.*, 2005, **5**, 1569–1574.
- T. A. Laurence, G. Braun, C. Talley, A. Schwartzberg, M. Moskovits, N. Reich and T. Huser, *J. Am. Chem. Soc.*, 2009, **131**, 162–169.
- C. Qiu, L. Zhang, H. Wang and C. Jiang, *J. Phys. Chem. Lett.*, 2012, **3**, 651–657.
- L. Zhang and H. Wang, *ACS Nano*, 2011, **5**, 3257–3267.
- C. M. S. Izumi, M. G. Moffitt and A. G. Brolo, *J. Phys. Chem. C*, 2011, **115**, 19104–19109.
- L. Piao, S. Park, H. B. Lee, K. Kim, J. Kim and T. D. Chung, *Anal. Chem.*, 2010, **82**, 447–451.
- C. L. Du, M. X. Yang, Y. M. You, T. Chen, H. Y. Chen and Z. X. Shen, *Chem. Phys. Lett.*, 2009, **473**, 317–320.
- S. L. Kleinman, J. M. Bingham, A.-I. Henry, K. L. Wustholz and R. P. Van Duyne, ed. M. I. Stockman, SPIE, San Diego, CA, 2010, pp. 77570–77510.
- M. Rycenga, X. H. Xia, C. H. Moran, F. Zhou, D. Qin, Z. Y. Li and Y. N. Xia, *Angew. Chem., Int. Ed.*, 2011, **50**, 5473–5477.
- W. E. Doering and S. M. Nie, *Anal. Chem.*, 2003, **75**, 6171–6176.
- D. S. Sebba, D. A. Watson and J. P. Nolan, *ACS Nano*, 2009, **3**, 1477–1484.
- S. W. Bishnoi, C. J. Rozell, C. S. Levin, M. K. Gheith, B. R. Johnson, D. H. Johnson and N. J. Halas, *Nano Lett.*, 2006, **6**, 1687–1692.
- R. A. Jensen, J. Sherin and S. R. Emory, *Appl. Spectrosc.*, 2007, **61**, 832–838.
- P. Mohanty, I. Yoon, T. Kang, K. Seo, K. S. K. Varadwaj, W. Choi, Q. H. Park, J. P. Ahn, Y. D. Suh, H. Ihee and B. Kim, *J. Am. Chem. Soc.*, 2007, **129**, 9576–9577.
- C. L. Du, Y. M. You and Z. X. Shen, *Opt. Commun.*, 2011, **284**, 5844–5846.
- B. J. Wiley, Y. C. Chen, J. M. McLellan, Y. J. Xiong, Z. Y. Li, D. Ginger and Y. N. Xia, *Nano Lett.*, 2007, **7**, 1032–1036.
- K. R. Krishnadas, P. R. Sajanlal and T. Pradeep, *J. Phys. Chem. C*, 2011, **115**, 4483–4490.
- D. P. Fromm, A. Sundaramurthy, A. Kinkhabwala, P. J. Schuck, G. S. Kino and W. E. Moerner, *J. Chem. Phys.*, 2006, **124**, 061101.
- N. Djaker, R. Hostein, E. Devaux, T. W. Ebbesen, H. Rigneault and J. Wenger, *J. Phys. Chem. C*, 2010, **114**, 16250–16256.
- H. Wei, U. Hakanson, Z. L. Yang, F. Hook and H. X. Xu, *Small*, 2008, **4**, 1296–1300.
- K. A. Homan, J. Chen, A. Schiano, M. Mohamed, K. A. Willets, S. Murugesan, K. J. Stevenson and S. Emelianov, *Adv. Funct. Mater.*, 2011, **21**, 1673–1680.
- C. Hrelescu, T. K. Sau, A. L. Rogach, F. Jackel and J. Feldmann, *Appl. Phys. Lett.*, 2009, **94**, 153113.
- J. Ye, C. Chen, L. Lagae, G. Maes, G. Borghs and P. Van Dorpe, *Phys. Chem. Chem. Phys.*, 2010, **12**, 11222–11224.
- D. A. Weitz and M. Oliveria, *Phys. Rev. Lett.*, 1984, **52**, 1433–1436.
- K. Kneipp, H. Kneipp, V. B. Kartha, R. Manoharan, G. Deinum, I. Itzkan, R. R. Dasari and M. S. Feld, *Phys. Rev. E: Stat. Phys., Plasmas, Fluids, Relat. Interdiscip. Top.*, 1998, **57**, R6281–R6284.
- P. H. C. Camargo, C. M. Cogley, M. Rycenga and Y. N. Xia, *Nanotechnology*, 2009, **20**, 434020.
- J. P. Camden, J. A. Dieringer, Y. M. Wang, D. J. Masiello, L. D. Marks, G. C. Schatz and R. P. Van Duyne, *J. Am. Chem. Soc.*, 2008, **130**, 12616–12617.
- M. Rycenga, P. H. C. Camargo, W. Y. Li, C. H. Moran and Y. N. Xia, *J. Phys. Chem. Lett.*, 2010, **1**, 696–703.
- K. Kim, D. Shin, K. L. Kim and K. S. Shin, *Phys. Chem. Chem. Phys.*, 2010, **12**, 3747–3752.
- J. Kumar and K. G. Thomas, *J. Phys. Chem. Lett.*, 2011, **2**, 610–615.
- T. Dadosh, J. Sperling, G. W. Bryant, R. Breslow, T. Shegai, M. Dyschel, G. Haran and I. Bar-Joseph, *ACS Nano*, 2009, **3**, 1988–1994.
- C. A. Tao, Q. An, W. Zhu, H. W. Yang, W. N. Li, C. X. Lin, D. Xu and G. T. Li, *Chem. Commun.*, 2011, **47**, 9867–9869.

- 65 A. McLintock, N. Hunt and A. W. Wark, *Chem. Commun.*, 2011, **47**, 3757–3759.
- 66 W. H. Park, S. H. Ahn and Z. H. Kim, *ChemPhysChem*, 2008, **9**, 2491–2494.
- 67 C. D. Geddes, H. Cao, I. Gryczynski, Z. Gryczynski, J. Y. Fang and J. R. Lakowicz, *J. Phys. Chem. A*, 2003, **107**, 3443–3449.
- 68 S. J. Lee, J. M. Baik and M. Moskovits, *Nano Lett.*, 2008, **8**, 3244–3247.
- 69 R. Sardar, T. B. Heap and J. S. Shumaker-Parry, *J. Am. Chem. Soc.*, 2007, **129**, 5356–5357.
- 70 W. Y. Li, P. H. C. Camargo, X. M. Lu and Y. N. Xia, *Nano Lett.*, 2009, **9**, 485–490.
- 71 K. D. Alexander, K. Skinner, S. P. Zhang, H. Wei and R. Lopez, *Nano Lett.*, 2010, **10**, 4488–4493.
- 72 E. K. Payne, K. L. Shuford, S. Park, G. C. Schatz and C. A. Mirkin, *J. Phys. Chem. B*, 2006, **110**, 2150–2154.
- 73 J. Fischer, N. Vogel, R. Mohammadi, H. J. Butt, K. Landfester, C. K. Weiss and M. Kreiter, *Nanoscale*, 2011, **3**, 4788–4797.
- 74 G. Chen, Y. Wang, M. X. Yang, J. Xu, S. J. Goh, M. Pan and H. Y. Chen, *J. Am. Chem. Soc.*, 2010, **132**, 3644–3645.
- 75 R. Gunawidjaja, S. Peleshanko, H. Ko and V. V. Tsukruk, *Adv. Mater.*, 2008, **20**, 1544–1549.
- 76 J. Theiss, P. Pavaskar, P. M. Echternach, R. E. Muller and S. B. Cronin, *Nano Lett.*, 2010, **10**, 2749–2754.
- 77 R. Kattumenu, C. H. Lee, L. M. Tian, M. E. McConney and S. Singamaneni, *J. Mater. Chem.*, 2011, **21**, 15218–15223.
- 78 Y. Bao, L. Vigderman, E. R. Zubarev and C. Jiang, *Langmuir*, 2012, **28**, 923–930.
- 79 K. H. Su, S. Durant, J. M. Steele, Y. Xiong, C. Sun and X. Zhang, *J. Phys. Chem. B*, 2006, **110**, 3964–3968.
- 80 P. R. Brejna, U. Sahayrn, M. G. Norton and P. R. Griffiths, *J. Phys. Chem. C*, 2011, **115**, 1444–1449.
- 81 G. Decher, *Science*, 1997, **277**, 1232–1237.
- 82 P. T. Hammond, *Adv. Mater.*, 2004, **16**, 1271–1293.
- 83 C. Y. Jiang and V. V. Tsukruk, *Adv. Mater.*, 2006, **18**, 829–840.
- 84 P. H. C. Camargo, M. Rycenga, L. Au and Y. N. Xia, *Angew. Chem., Int. Ed.*, 2009, **48**, 2180–2184.
- 85 P. H. C. Camargo, L. Au, M. Rycenga, W. Y. Li and Y. N. Xia, *Chem. Phys. Lett.*, 2010, **484**, 304–308.
- 86 M. Rycenga, M. H. Kim, P. H. C. Camargo, C. Cobley, Z. Y. Li and Y. N. Xia, *J. Phys. Chem. A*, 2009, **113**, 3932–3939.
- 87 S. Y. Lee, L. Hung, G. S. Lang, J. E. Cornett, I. D. Mayergoyz and O. Rabin, *ACS Nano*, 2010, **4**, 5763–5772.
- 88 X. Y. Xu, K. Seal, X. S. Xu, I. Ivanov, C. H. Hsueh, N. Abu Hatab, L. F. Yin, X. Q. Zhang, Z. H. Cheng, B. H. Gu, Z. Y. Zhang and J. A. Shen, *Nano Lett.*, 2011, **11**, 1265–1269.
- 89 C. F. Tian, C. H. Ding, S. Y. Liu, S. C. Yang, X. P. Song, B. J. Ding, Z. Y. Li and J. X. Fang, *ACS Nano*, 2011, **5**, 9442–9449.
- 90 A. Dhawan, S. J. Norton, M. D. Gerhold and T. Vo-Dinh, *Opt. Express*, 2009, **17**, 9688–9703.
- 91 T. Kang, I. Yoon, K. S. Jeon, W. Choi, Y. Lee, K. Seo, Y. Yoo, Q. H. Park, H. Ihee, Y. D. Suh and B. Kim, *J. Phys. Chem. C*, 2009, **113**, 7492–7496.
- 92 Y. Wu and P. Nordlander, *J. Phys. Chem. C*, 2010, **114**, 7302–7307.
- 93 I. Yoon, T. Kang, W. Choi, J. Kim, Y. Yoo, S. W. Joo, Q. H. Park, H. Ihee and B. Kim, *J. Am. Chem. Soc.*, 2009, **131**, 758–762.
- 94 M. Becker, V. Sivakov, G. Andrä, R. Geiger, J. Schreiber, S. Hoffmann, J. Michler, A. P. Milenin, P. Werner and S. H. Christiansen, *Nano Lett.*, 2007, **7**, 75–80.
- 95 M. A. Khan, T. P. Hogan and B. Shanker, *J. Raman Spectrosc.*, 2008, **39**, 893–900.
- 96 N. L. Netzer, R. Gunawidjaja, M. Hiemstra, Q. Zhang, V. V. Tsukruk and C. Y. Jiang, *ACS Nano*, 2009, **3**, 1795–1802.
- 97 M. K. Gupta, S. Chang, S. Singamaneni, L. F. Drummy, R. Gunawidjaja, R. R. Naik and V. V. Tsukruk, *Small*, 2011, **7**, 1192–1198.
- 98 R. Gunawidjaja, E. Kharlampieva, I. Choi and V. V. Tsukruk, *Small*, 2009, **5**, 2460–2466.
- 99 H. Wei, F. Hao, Y. Z. Huang, W. Z. Wang, P. Nordlander and H. X. Xu, *Nano Lett.*, 2008, **8**, 2497–2502.
- 100 Y. R. Fang, H. Wei, F. Hao, P. Nordlander and H. X. Xu, *Nano Lett.*, 2009, **9**, 2049–2053.
- 101 S. Chang, H. Ko, R. Gunawidjaja and V. V. Tsukruk, *J. Phys. Chem. C*, 2011, **115**, 4387–4394.
- 102 E. C. Garnett, W. Cai, J. J. Cha, F. Mahmood, S. T. Connor, M. Greyson Christoforo, Y. Cui, M. D. McGehee and M. L. Brongersma, *Nat. Mater.*, 2012, **11**, 241–249.
- 103 H. P. Yoon, M. M. Maitani, O. M. Cabarcos, L. T. Cai, T. S. Mayer and D. L. Allara, *Nano Lett.*, 2010, **10**, 2897–2902.
- 104 O. J. Glembocki, R. W. Rendell, D. A. Alexson, S. M. Prokes, A. Fu and M. A. Mastro, *Phys. Rev. B: Condens. Matter Mater. Phys.*, 2009, **80**, 085416.
- 105 M. Zhang, S. L. Fang, A. A. Zakhidov, S. B. Lee, A. E. Aliev, C. D. Williams, K. R. Atkinson and R. H. Baughman, *Science*, 2005, **309**, 1215–1219.
- 106 F. Le, N. Z. Lwin, N. J. Halas and P. Nordlander, *Phys. Rev. B: Condens. Matter Mater. Phys.*, 2007, **76**, 165410.
- 107 W. H. Park and Z. H. Kim, *Nano Lett.*, 2010, **10**, 4040–4048.
- 108 T. Vo-Dinh, *Trends Anal. Chem.*, 1998, **17**, 557–582.
- 109 M. Fleischmann, P. J. Hendra and A. J. McQuillan, *Chem. Phys. Lett.*, 1974, **26**, 163–166.
- 110 C. Y. Chen and E. Burstein, *Phys. Rev. Lett.*, 1980, **45**, 1287–1291.
- 111 P. L. Stiles, J. A. Dieringer, N. C. Shah and R. R. Van Duyne, *Annu. Rev. Anal. Chem.*, 2008, **1**, 601–626.
- 112 J. P. Goudonnet, J. L. Bijeon, R. J. Warmack and T. L. Ferrell, *Phys. Rev. B: Condens. Matter*, 1991, **43**, 4605.
- 113 J. J. Mock, R. T. Hill, A. Degiron, S. Zauscher, A. Chilkoti and D. R. Smith, *Nano Lett.*, 2008, **8**, 2245–2252.
- 114 M. Hu, A. Ghoshal, M. Marquez and P. G. Kik, *J. Phys. Chem. C*, 2010, **114**, 7509–7514.
- 115 L. Vigderman and E. R. Zubarev, *Langmuir*, 2012, DOI: 10.1021/la300218z.
- 116 H. Gehan, L. Fillaud, M. M. Chehimi, J. Aubard, A. Hohenau, N. Felidj and C. Mangeney, *ACS Nano*, 2010, **4**, 6491–6500.
- 117 A. M. Schwartzberg, C. D. Grant, A. Wolcott, C. E. Talley, T. R. Huser, R. Bogomolni and J. Z. Zhang, *J. Phys. Chem. B*, 2004, **108**, 19191–19197.
- 118 S. Sasic, T. Itoh and Y. Ozaki, *J. Raman Spectrosc.*, 2005, **36**, 593–599.
- 119 J. Q. Zhuang, H. M. Wu, Y. G. Yang and Y. C. Cao, *Angew. Chem., Int. Ed.*, 2008, **47**, 2208–2212.
- 120 N. Gandra, A. Abbas, L. Tian and S. Singamaneni, *Nano Lett.*, 2012, **12**, 2645–2651.
- 121 Y. Kitahama, A. Ogawa, Y. Tanaka, S. Obeidat, T. Itoh, M. Ishikawa and Y. Ozaki, *Chem. Phys. Lett.*, 2010, **493**, 309–313.
- 122 H. W. Tang, X. B. Yang, J. Kirkham and D. A. Smith, *Anal. Chem.*, 2007, **79**, 3646–3653.
- 123 C. Y. Jiang, W. Y. Lio and V. V. Tsukruk, *Phys. Rev. Lett.*, 2005, **95**, 115503.
- 124 C. Y. Jiang, S. Markutsya, H. Shulha and V. V. Tsukruk, *Adv. Mater.*, 2005, **17**, 1669–1673.
- 125 N. Pazos-Perez, W. H. Ni, A. Schweikart, R. A. Alvarez-Puebla, A. Fery and L. M. Liz-Marzan, *Chem. Sci.*, 2010, **1**, 174–178.
- 126 D. K. Lim, K. S. Jeon, J. H. Hwang, H. Kim, S. Kwon, Y. D. Suh and J. M. Nam, *Nat. Nanotechnol.*, 2011, **6**, 452–460.
- 127 H. Qi, D. Alexson, O. Glembocki and S. M. Prokes, *Nanotechnology*, 2010, **21**, 085705.
- 128 C. Fang, A. Agarwal, E. Widjaja, M. V. Garland, S. M. Wong, L. Linn, N. M. Khalid, S. M. Salim and N. Balasubramanian, *Chem. Mater.*, 2009, **21**, 3542–3548.
- 129 C. H. Lee, L. M. Tian, A. Abbas, R. Kattumenu and S. Singamaneni, *Nanotechnology*, 2011, **22**, 275311.
- 130 N. L. Netzer, C. Qiu, Y. Y. Zhang, C. K. Lin, L. F. Zhang, H. Fong and C. Y. Jiang, *Chem. Commun.*, 2011, **47**, 9606–9608.
- 131 C. Liusman, S. Z. Li, X. D. Chen, W. Wei, H. Zhang, G. C. Schatz, F. Boey and C. A. Mirkin, *ACS Nano*, 2010, **4**, 7676–7682.
- 132 J. X. Fang, S. Y. Du, S. Lebedkin, Z. Y. Li, R. Kruk, M. Kappes and H. Hahn, *Nano Lett.*, 2010, **10**, 5006–5013.
- 133 J. X. Fang, S. Lebedkin, S. C. Yang and H. Hahn, *Chem. Commun.*, 2011, **47**, 5157–5159.
- 134 D. Xu, J. J. Gu, W. N. Wang, X. C. Yu, K. Xi and X. D. Jia, *Nanotechnology*, 2010, **21**, 375101.
- 135 Y. Y. Jiang, X. J. Wu, Q. Li, J. J. Li and D. S. Xu, *Nanotechnology*, 2011, **22**, 385601.
- 136 H. Wang and N. J. Halas, *Adv. Mater.*, 2008, **20**, 820–825.
- 137 H. Y. Liang, Z. P. Li, W. Z. Wang, Y. S. Wu and H. X. Xu, *Adv. Mater.*, 2009, **21**, 4614–4618.

- 
- 138 J. P. Xie, Q. B. Zhang, J. Y. Lee and D. I. C. Wang, *ACS Nano*, 2008, **2**, 2473–2480.
- 139 J. X. Fang, S. Y. Liu and Z. Y. Li, *Biomaterials*, 2011, **32**, 4877–4884.
- 140 K. G. Laurier, M. Poets, F. Vermoortele, G. De Cremer, J. A. Martens, H. Uji-i, D. E. De Vos, J. Hofkens and M. B. Roeffaers, *Chem. Commun.*, 2012, **48**, 1559–1561.
- 141 J. H. Hong, Y. K. Hwang, J. Y. Hong, H. J. Kim, S. J. Kim, Y. S. Won and S. Huh, *Chem. Commun.*, 2011, **47**, 6963–6965.
- 142 D. Han, S. Y. Lim, B. J. Kim, L. Piao and T. D. Chung, *Chem. Commun.*, 2010, **46**, 5587–5589.
- 143 G. L. Liu, Y. Lu, J. Kim, J. C. Doll and L. P. Lee, *Adv. Mater.*, 2005, **17**, 2683–2688.
- 144 G. Goddard, L. O. Brown, R. Habbersett, C. I. Brady, J. C. Martin, S. W. Graves, J. P. Freyer and S. K. Doorn, *J. Am. Chem. Soc.*, 2010, **132**, 6081–6090.
- 145 M. P. Cecchini, M. A. Stapountzi, D. W. McComb, T. Albrecht and J. B. Ediel, *Anal. Chem.*, 2011, **83**, 1418–1424.